Inorganic Chemistry
Article

Inorg. Chem. **2010**, *49*, 10067–10073 **10067**
DOI: 10.1021/ic101414x

Autogenic Synthesis of Green- and Red-Emitting Single-Phase $Pr_2O_2CO_3$ and $PrO_{1.833}$ Luminescent Nanopowders

Jose M. Calderon Moreno,*,† Vilas G. Pol,‡ Soong-Hyuck Suh,§ and Monica Popa†

†*Institute of Physical Chemistry Ilie Murgulescu, Romanian Academy, Splaiul Independentei 202, Bucharest 060021, Romania,* ‡*Electrochemical Energy Storage Department, Chemical Sciences and Engineering Division, Argonne National Laboratory, 9700 S. Cass Avenue, Argonne, Illinois 60439, and* §*Department of Chemical Engineering, Keimyung University, Daegu 704-701, Korea*

Received July 15, 2010

This Article reveals a rare synthesis of pure $Pr_2O_2CO_3$ (POC) nanopowder by thermolysis (700 °C) of a single chemical precursor in an autogenic reaction. The autogenic thermolysis of praseodymium acetate is a solvent-free, efficient, and straightforward approach yielding luminescent POC nanoparticles. The as-prepared POC nanopowder converted to $PrO_{1.833}$ (PO) powder via combustion. Methodical morphological, structural, and compositional characterizations of POC and PO powders are carried out, supported by mechanistic elucidation and the photoluminescent properties.

Introduction

Rare-earth ion (REI) oxides or REI-doped materials are of great importance because of their wide range of applications in lasers, optical amplifiers, and optical sensors.[1] The energy level structure of the Pr^{3+} ion allows many linear and nonlinear effects, such as UV-tunable luminescence from low-lying 4f−5d levels,[2] visible emission from either $^3P_0$ or $^1D_2$ levels, etc., giving rise to greenish-blue or red luminescences.[3] The size and shape control of the phosphor, crystalline nature, and activator homogeneity are of great importance for determining the luminescent properties of REI.[4] Generally, phosphors with larger particle size are good for improvement of the photoluminescence (PL) intensity.[5] Wang et al.[4] showed a decrease in the PL intensity with a decrease in the crystallite size. On the other hand, the depth of penetration of low-energy electron beams is approximately 10 nm for field-emission displays.[6] Therefore, nanosized phosphors are more cost-effective and necessary than commercially available microsized ones in low-voltage operation.[7]

There are limited reports in the literature on the synthesis of Pr^{3+} ion related materials. The praseodymium ions were embedded in SiO_2/TiO_2 glasses by the sol−gel method, and PL excitation spectra revealed the presence of energy transfer between the host matrix states and the Pr^{3+} ions.[8] The praseodymium oxide formation by thermal decomposition of a praseodymium carbonate octahydrate was demonstrated by Popa and Kakihana.[9] Luminescent one-dimensional nanostructured praseodymium oxyfluoride was carried out via electrospinning of a mixture of praseodymium trifluoroacetic acid/poly(vinylpyrrolidone) followed by calcination.[10] ZrO_2/Pr films were synthesized by the ultrasonic spray pyrolysis process, and the PL properties of the films were studied as a function of the substrate temperature and the praseodymium concentration.[11] Determination of Pr^{III} ions and its 4f luminescence was also studied in solutions of mixed-ligand complexes with fluorinated β-diketones and donor active ligands.[12]

*To whom correspondence should be addressed. E-mail: josecalderonmoreno@yahoo.com. Tel: + 40.21.316.79.12. Fax: + 40.21.312.11.47.

(1) Digonnet, M. J. F. *Rare Earth Doped Fiber Lasers and Amplifiers*; Dekker: New York, 1993.
(2) Nicolas, S.; Laroche, M.; Girard, S.; Moncorgé, R.; Guyot, Y.; Joubert, M. F.; Descroix, E.; Petrosyan, A. G. *J. Phys.: Condens. Matter* **1999**, *11*, 7937.
(3) Kaminskii, A. A. In *Advanced Solid State Lasers*, New Orleans, LA, Feb 1−3, 1993; Pinto, A., Fan, T. Y., Eds.; Optical Society of America: Washington, DC, 1993; Vol. *15*,
(4) Wang, W. N.; Widiyastuti, W.; Ogi, T.; Wuled Lenggoro, I.; Okuyama, K. *Chem. Mater.* **2007**, *19*, 1723.
(5) Jing, X.; Ireland, T. G.; Gibbons, C.; Barber, D. J.; Silver, J.; Vecht, A.; Fern, G.; Trogwa, P.; Morton, D. *J. Electrochem. Soc.* **1999**, *146*, 4654.
(6) Hakuta, Y.; Haganuma, T.; Sue, K.; Adschiri, T.; Arai, K. *Mater. Res. Bull.* **2003**, *38*, 1257.
(7) Amlouka, A.; Mira, L.; Kraiem, S.; Saadoun, M.; Alaya, S.; Pierre, A. C. *Mater. Sci. Eng., B* **2008**, *146*, 74.
(8) Jeon, B. S.; Kang, S. W.; Yoo, J. S.; Lee, J. D. Characterization of low-voltage phosphor screens for fed applications. In *Flat Panel Display Materials II*; Hatalis, M. K., Kanicki, J., Summers, C. J., Funada, F., Eds.; Materials Research Society Symposium Proceedings 424; Materials Research Society: Pittsburgh, PA, 1997; pp 421−424.
(9) Popa, M.; Kakihana, M. *Solid State Ionics* **2001**, *141−142*, 265.
(10) Wang, H.; Yang, Y.; Wang, Y.; Li, X.; Feng, S.; Wang, C. *Mater. Sci. Eng., B* **2008**, *147*, 69.
(11) Ramos-Brito, F.; Garcıa-Hipolito, M.; Alejo-Armenta, C.; Alvarez-Fragoso, O.; Falcony, C. *J. Phys. D: Appl. Phys.* **2007**, *40*, 6718.
(12) Meshkova, S. B.; Kiriyak, A. V.; Topilova, Z. M.; Antonovich, V. P. *J. Anal. Chem.* **2007**, *62*, 362.

Published on Web 10/05/2010

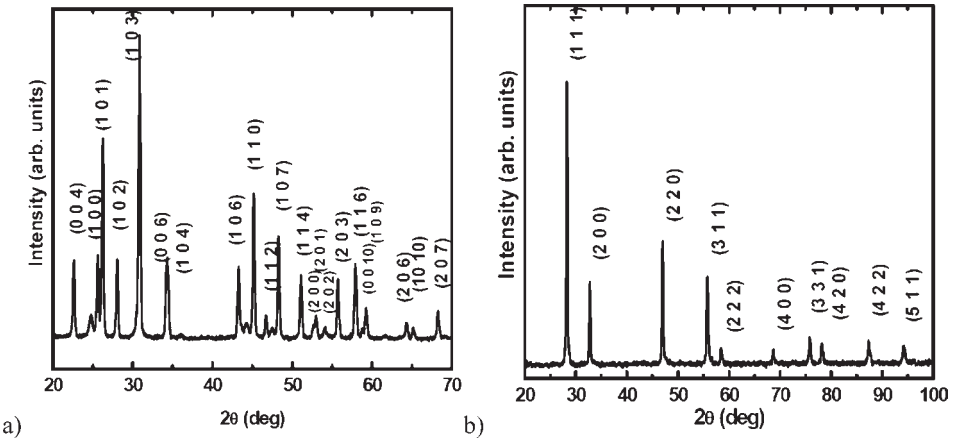

Figure 1. XRD patterns of (a) POC and (b) PO samples.

Photoacoustic spectroscopy to evaluate the nonradiative transition of Pr^{3+} in ZnO powders with various praseodymium concentrations and sintering temperatures was studied by Inoue et al.[13]

According to our literature search, there are no reports on the synthesis of pure $Pr_2O_2CO_3$ (POC) nanoparticles, eventually on their PL studies. Shrestha et al.[14] reported the synthesis of $PrO_{1.833}$ (PO) nanoparticles obtained by precipitation of a praseodymium nitrate solution. The present research demonstrates a solvent-free, efficient synthesis process to prepare luminescent nanoparticles of POC. Thermolysis of a single precursor, praseodymium acetate, at 700 °C in a closed reactor under autogenic pressure yields POC. The as-prepared POC nanoparticles were further heated in air to 700 °C to facilitate the fabrication of PO nanoparticles. Systematic morphological, structural, and compositional characterizations of POC and PO nanoparticles are carried out, and the PL properties are studied.

Experimental Section

Praseodymium acetate [PA; $Pr(O_2C_2H_3)_3$] was purchased from Sigma-Aldrich and used as received. In a typical synthesis of POC particles, 1 g of PA was introduced in a 5 cm^3 specially designed reactor (made of Haynes 230 alloy) at room temperature in an inert nitrogen atmosphere. The partially filled reactor with PA was closed tightly and placed at the center of a furnace for uniform heating. The temperature of the furnace was ramped up to 700 °C at a rate of 30 °C/min and maintained at that temperature for 1 h. The maximum pressure of ~2 MPa was measured at 700 °C during thermal dissociation of PA. A total of 0.52 g of powder was obtained upon natural cooling of the reactor to room temperature. The as-prepared POC nanoparticles were further heated to 700 °C in air to facilitate synthesis of the PO particles. Both products were directly characterized for their morphological, compositional, structural, and PL properties. The phase purity and crystal structure of POC and PO were determined using X-ray diffraction (XRD) and IR and Raman spectroscopy. The XRD pattern was recorded by using a Bruker AXSD* Advance powder X-ray diffractometer (Cu Kα radiation, wavelength 1.5406 Å). The Raman spectra were recorded at room temperature by using a triple Jobin Yvon/Atago-Bussan T-6400 spectrometer, equipped with an

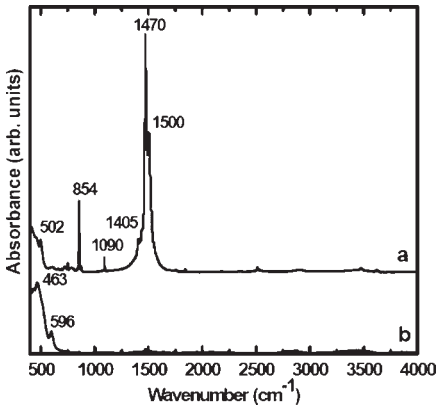

Figure 2. FT-IR spectra of (a) POC and (b) PO powders.

Ar^+ laser (λ = 514.5 nm) and a liquid-nitrogen-cooled CCD detector. Scanning electron microscopy (SEM) characterization was carried out in Zeiss EVO L10 and Jeol JSM-840 microscopes equipped with a INCA Energy 250 (Oxford Instruments) energy-dispersive (EDS) X-ray system. The IR spectra of POC and PO were obtained at a resolution of 2 cm^{-1}, over a frequency range from 4000 to 400 cm^{-1}, using a Perkin-Elmer model spectrophotometer. The spectra were taken from thin (~20 mg/cm^2) KBr pellets containing samples of ~1 wt %. Pellets were prepared by compacting an intimate mixture obtained by grinding 1 mg of the substance in 100 mg of KBr powder. PL measurements were carried out using a fluorescence spectrometer. Filters were used so as to select the 510−520 nm wavelength region of the spectra of a tungsten white-light source as the excitation source, and the emission signal was collected in an Olympus microscope through an objective with 50× magnification.

Results and Discussion

The XRD pattern (shown in Figure 1a) of POC corresponds to a hexagonal type II polymorph of praseodymium oxycarbonate (JCPDS file 37-0805; space group *P*63/*mmc*) and is in good agreement with other isostructural oxycarbonates ($Gd_2O_2CO_3$, $Sm_2O_2CO_3$, $Y_2O_2CO_3$,[15] and $La_2O_2CO_3$[16]). Additionally, the XRD pattern of POC matches very well with the recently reported $Eu_2O_2CO_3$ superstructures fabricated by a

(13) Inoue, Y.; Okamoto, M.; Kawahara, T.; Morimoto, J. *J. Alloys Compd.* **2006**, *408*−*412*, 1234.
(14) Shrestha, S.; Yeung, C. M. Y.; Mills, C. E.; Lewington, J.; Tsang, S. C. *Angew. Chem., Int. Ed.* **2007**, *46*, 3855.
(15) Imanaka, N.; Masui, T.; Mayama, Y.; Koyabu, K. *J. Solid State Chem.* **3601**, *178*, 2005.
(16) Koyabu, K.; Masui, T.; Tamura, S.; Imanaka, N. *J. Alloys Compd.* **2006**, *408*, 867.

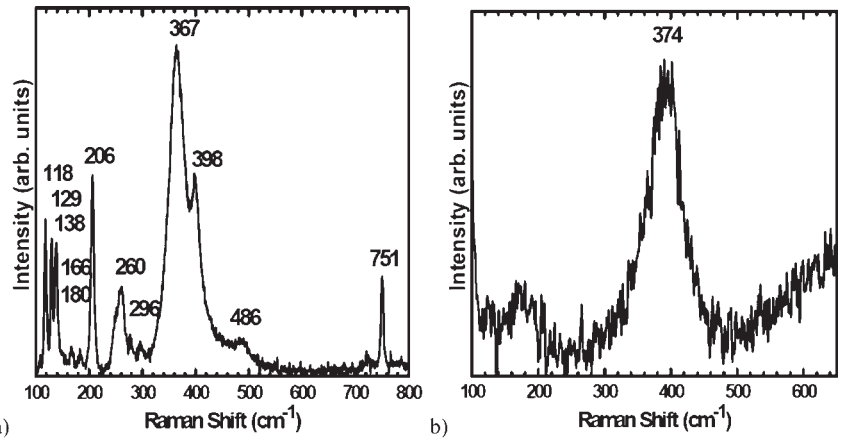

Figure 3. Raman spectra of (a) POC and (b) PO powders.

single-step autogenic reaction.[17] The XRD pattern confirms that single-phase oxycarbonate of praseodymium is obtained without any impurity peaks. The further combustion of POC particles at 700 °C in air facilitated the synthesis of PO particles (Figure 1b). The strong support for the formation of PO was provided by XRD lines, which display only the pattern according to JCPDS 6-329 corresponding to this type of praseodymium oxide, with a body-centered-cubic structure indicating the complete conversion of the oxycarbonate into praseodymium oxide. Praseodymium oxides comprise stoichiometric Pr_2O_3 and PrO_2, as well as nonstoichiometric oxides, PrO_x (x = 1.833, 1.810, 1.780, 1.714, and 1.67).[9,11] Stoichiometric oxides adopt hexagonal, Pr_2O_3, and fluorite, PrO_2, structures, whereas nonstoichiometric ones are oxygen-deficient modifications of the fluorite structure.[9,18,19] Praseodymium oxide $PrO_{1.833}$ (or Pr_6O_{11}) is usually produced via thermal decomposition of many salts such as acetate,[18] oxalate,[19] formate,[20] nitrate,[21] adipate and sebacate,[22] and citrate.[9,18] The observed phases depend on the precursor used, the atmosphere, and the temperature of decomposition. Thermal decomposition of praseodymium acetate has been studied briefly. Like many other rare-earth carboxylates, thermal decomposition proceeds via the formation of oxycarbonate as an intermediate, leading eventually to the formation of the metal oxide.[9,18,19] In our case, at 700 °C, the final decomposition product from the praseodymium oxycarbonate was PO.

Moreover, the IR spectroscopy results confirm the phases mentioned above. The IR spectra of the POC and PO powders are shown in Figure 2. The spectrum recorded for the POC sample reveals the presence of absorptions at 1500−500 cm^{-1}, with bands located at 1500, 1470, 1405 (small shoulder), 1090, 854, and 502 cm^{-1}. Except the last absorption band, all of the other vibrations are due to the oxycarbonate band structure.[18−22] The bands below 850 cm^{-1} are related to metal−oxygen vibrations (lattice modes) of (Pr−O); thus, the band at 502 cm^{-1} is attributed to the Pr−O lattice vibration mode in POC. The absorption bands for the POC sample treated at 700 °C, located at 463 and 596 cm^{-1}, are related to the lattice vibration modes of Pr−O in PO. Moreover, the IR spectrum of the solid product at 700 °C shows no detectable absorption bands due to oxycarbonate species. The IR data prove that oxycarbonate decomposition takes place at this temperature, with total transformation into praseodymium oxide.

The IR spectroscopy results were completed by Raman spectroscopy studies. The Raman spectra of POC and PO powders are shown in Figure 3a,b. The Raman spectrum of the hexagonal polymorph of POC (in Figure 3a) shows a sharp band at 206 cm^{-1}, a stronger and broader feature at 367 cm^{-1}, and other less intense peaks at 118, 129, 138, 166, 180, 176, 206, 260, 290, 398, 486, and 751 cm^{-1}. All of the observed bands are attributed to single-phase POC. It must be indicated that we have not found any Raman data for praseodymium oxycarbonates in the literature, and the detailed analysis and band assignment of the first reported POC Raman spectrum exceeds the scope of this study.

The Raman spectrum of the PO powder is quite different because it shows only a strong feature as a wide band at 374 cm^{-1}. Some reports are available on Raman studies of rare-earth oxides in the bulk form,[23−29] but to the best of our knowledge, there are no reported Raman studies on the praseodymium-based oxides. Praseodymium dioxide, PrO_2, with Pr ions in a valence state of 4+, crystallizes in the cubic fluorite-type lattice and belongs to the space group O_h^5 ($Fm3m$). Group theoretical analysis predicts only one triply degenerate Raman-active optical phonon with F_{2g} symmetry, which can be viewed as a symmetric breathing mode of the O atoms around each cation, and two IR-active phonons of F_{1u} symmetry corresponding to the LO and TO modes. Because only the O atoms move, the mode frequency should be nearly independent of the cation mass and the spectrum should be similar to those of other fluorite-type single oxides, i.e., CeO_2,

(17) Pol, V. G.; Calderon-Moreno, J. M.; Popa, M.; Acharya, S.; Ariga, K.; Thiyagarajan, P. *Inorg. Chem.* **2009**, *48*, 5569.
(18) Popa, M.; Kakihana, M. *J. Therm. Anal. Calorim.* **2001**, *65*, 281.
(19) Hussein, G. A. M. *J. Anal. Appl. Pyrolysis* **1996**, *37*, 111.
(20) Masuda, Y. *Thermochim. Acta* **1983**, *67*, 271.
(21) Hussein, G. A. M.; Balboul, B. A. A.; Warith, M. A.; Othman, A. G. M. *Thermochim. Acta* **2001**, *369*, 59.
(22) Goldsmith, J. A.; Ross, S. D. *Spectrochim. Acta, Part A* **1967**, *23*, 1909.
(23) Tucker, L. A.; Karney, F. J., Jr.; McMillan, P.; Lin, S. H.; Lyring, L. *Appl. Spectrosc.* **1984**, *38*, 857.
(24) Urben Marek, W.; Cornilsen Bahn, C. *J. Phys. Chem. Solids* **1984**, *48*, 475.
(25) Lejus, A. M.; Michel, D. *Phys. Status Solidi B* **1977**, *84*, K105.
(26) Repelin, Y.; Proust, C.; Husson, E.; Benny, J. M. *J. Solid State Chem.* **1995**, *118*, 163.
(27) White, W. B.; Keramidas, V. G. *Spectrochim. Acta* **1972**, *28A*, 501.
(28) Keramidas, V. G.; White, W. B. *J. Chem. Phys.* **1973**, *59*, 1561.
(29) Dilawar, N.; Mehrotra, S.; Varandani, D.; Kumaraswamy, B. V.; Haldar, S. K.; Bandyopadhyay, A. K. *Mater. Charact.* **2008**, *59*, 462.

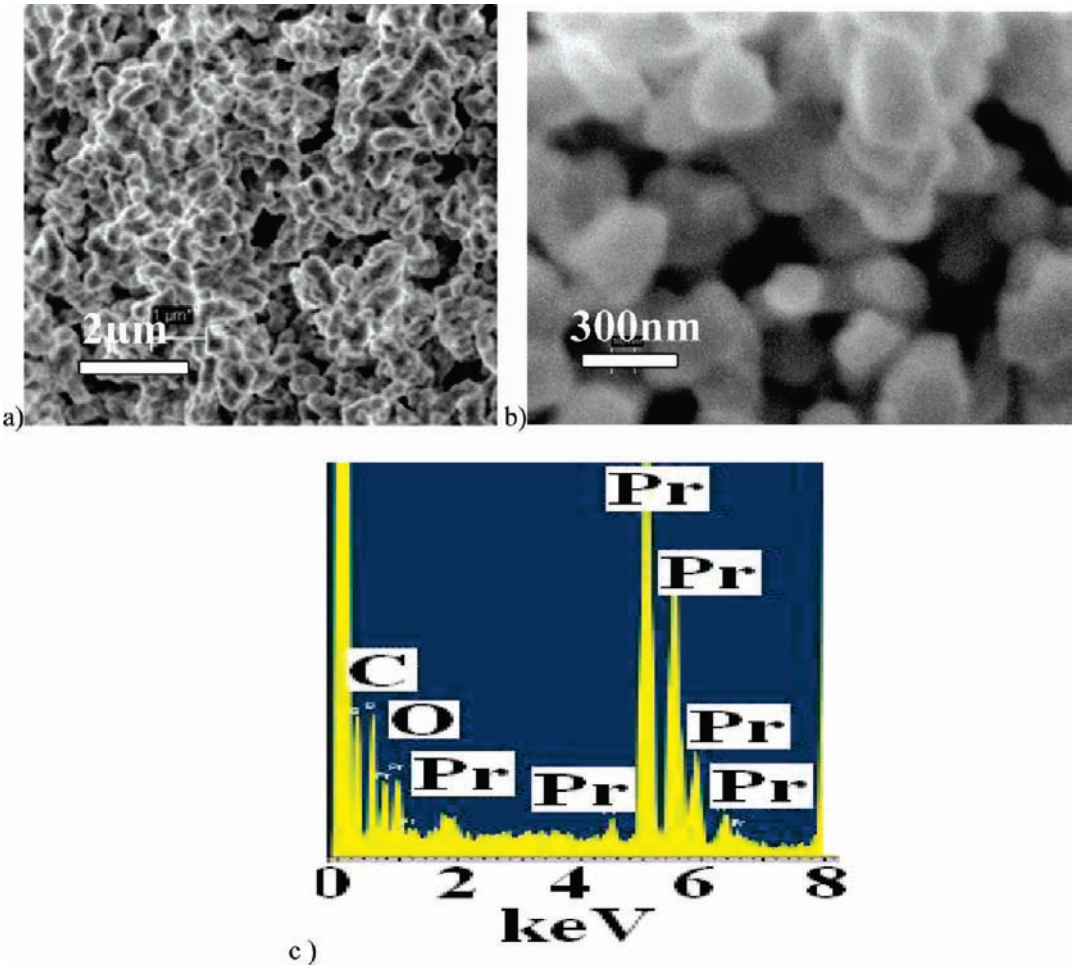

Figure 4. (a and b) SEM and (c) EDS of the POC powder.

for which the Raman spectrum is very simple and consists of only one intense Raman mode at ~465 cm^{-1}.

Praseodymium sesquioxide, Pr_2O_3, on the other hand, with Pr ions in a valence state of 3+, and other rare-earth sesquioxides with C-type structure crystallize in the body-centered-cubic lattice and belong to the space group $Ia3$ (T_h^7). The unit cell contains two primitive cells having eight formula units. Factor group analysis predicts a total of 22 Raman-active modes distributed as $^4A_g + {}^4E_g + {}^{14}F_g$. The ambient Raman spectrum and the different mode frequencies of both F-type CeO_2 and C-type RE_2O_3 have been reported in the literature for several rare earths (not for Pr). The measured Raman spectra of C-type rare-earth sesquioxides exhibit a characteristic strong feature at ~340−395 cm^{-1}.[23−29] The position of this Raman band is related to the strength of the RE−O bond and, for Pr_2O_3, extrapolating from other rare-earth Raman data, can be expected to be at ~370 cm^{-1}.

The only mode observed in the PO powder is a wide band at ~375 cm^{-1}, with some other very weak bands of low intensity and poor signal-to-noise ratio. Thus, the Raman spectrum has a profile similar to C-type RE_2O_3[27−29] or Y_2O_3,[30] except for the clear widening of the single main feature, compared to the spectra of nanosized rare-earth sesquioxides reported by Dilawar et al.[31] This widening is attributed to the mixed valence of Pr_6O_{11}. The PO structure is a modification from the fluorite structure, where Pr^{3+} cations have replaced Pr^{4+} at random in one out of every three cation lattice positions ($^1/_3$ of the lattice), introducing O^{2-} vacancies into the anionic sublattice. It is well-known that the Raman signal is affected by these randomly oriented vacancies that distort long-range ordering. The defect formation is a known source of structural disorder, and thus breakdown of the translational symmetry occurs, which results in relaxation of the $k \approx 0$ selection rule for Raman scattering, and hence phonons from all parts of the Brillouin zone contribute to the spectra.[32] This explains the absence of characteristic peaks of the fluorite-type spectrum, an effect very well-known in similar F-type + C-type systems, such as, for example, in cubic yttria-stabilized zirconia,[30] and causes also a wide broadening of the only observed Raman mode of Pr_2O_3 at 375 cm^{-1}, which is characteristic of the C-type mode. The absence of a mixed feature of both C-type and F-type oxides indicates a single-phase structure, where the long and short order in the anion lattice of PrO_2 is disrupted by the massive amount of random oxygen vacancies, without clustering of different praseodymium oxides, as was determined by XRD results.

(30) Phillippi, C. M.; Maazdiyasni, K. S. *J. Am. Ceram. Soc.* **1971**, *54*, 254.
(31) Calderon-Moreno, J. M.; Yoshimura, M. *Solid State Ionics* **2002**, *154*, 125.
(32) Calderon-Moreno, J. M.; Yoshimura, M. *Solid State Ionics* **2001**, *141−142*, 343.

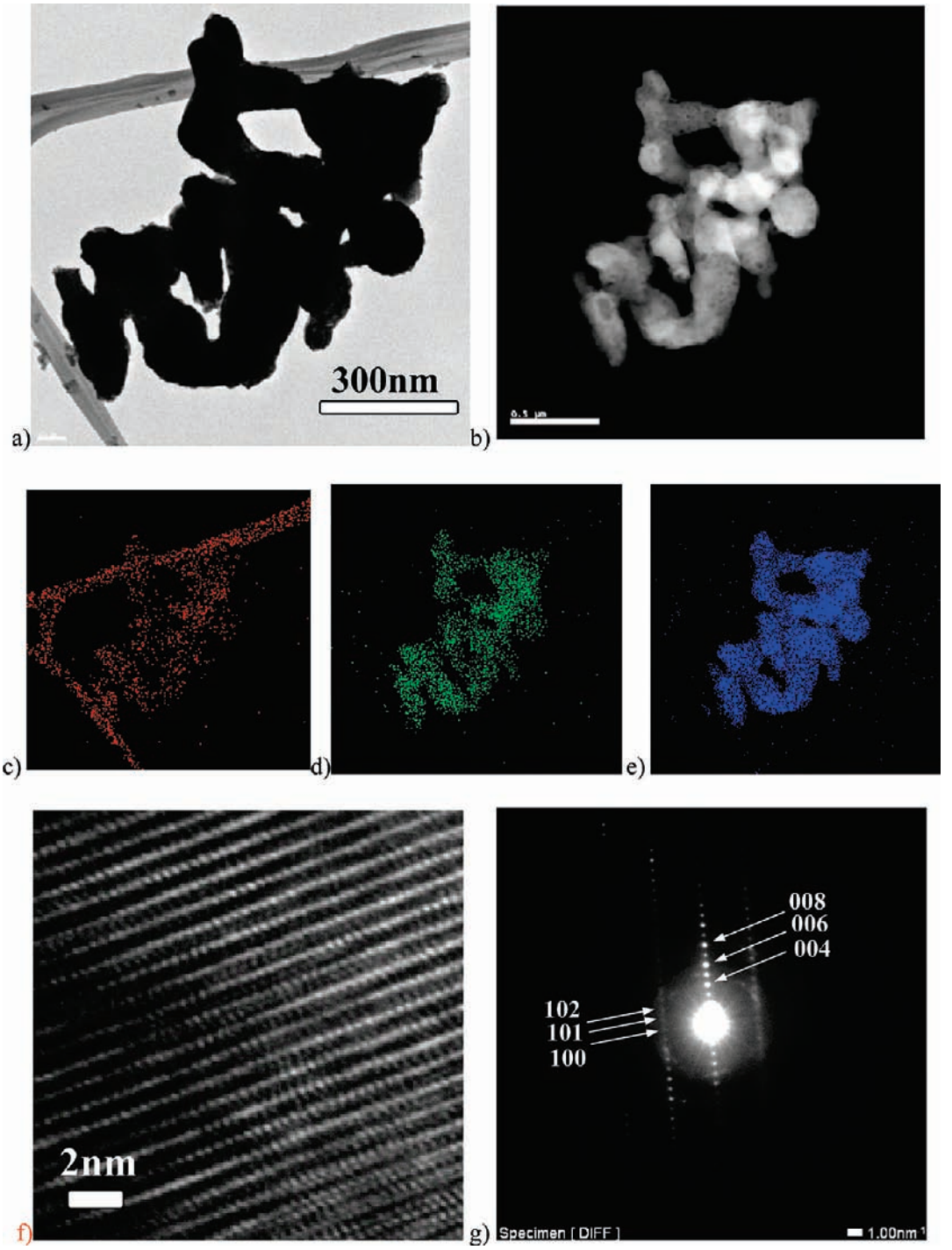

Figure 5. (a and b) Bright- and dark-field TEM images of POC, composition of (c) carbon, (d) praseodymium, and (e) oxygen, (f) HRTEM, and (g) electron diffraction.

Therefore, from both IR and XRD measurements as well as Raman evidence, we can assume the formation of praseodymium oxide after POC decomposition.

Parts a and b of Figure 4 depict SEM micrographs of the POC sample. Particles of 100−200 nm in size are formed during the autogenic thermal dissociation of PA. The elemental composition of POC particles is demonstrated in Figures 4c and 5. Transmission electron microscopy (TEM) and high-resolution TEM (HRTEM) were employed to obtain information about the structure of the obtained powders. The TEM of POC is presented in Figure 5; parts a and b of Figure 5 depict the particles selected for elemental dot mapping in bright- and dark-field images. Particles with dimensions of around 100 nm and connected with each other are formed. Two carbon fibers from the supported TEM grid on both sides of the particles are also observed in Figure 5a. Figure 5c shows elemental carbon dot mapping; the two-sided strands are aroused from the supported TEM grid. Parts d and e of Figure 5 depict the praseodymium and oxygen components, respectively. From elemental dot mapping, it is confirmed that the particles are composed of carbon, praseodymium, and

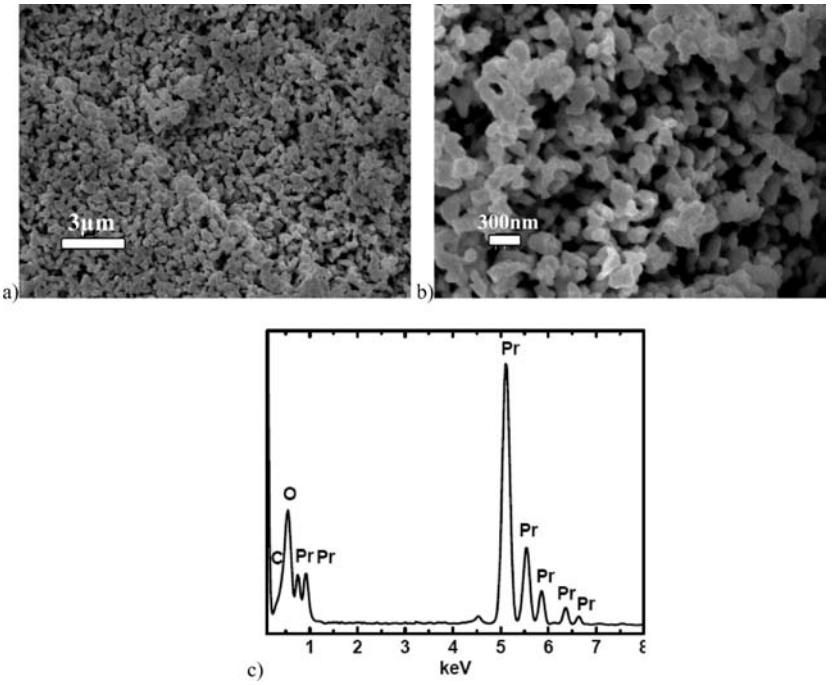

Figure 6. (a and b) SEM and (c) EDS of the PO powder.

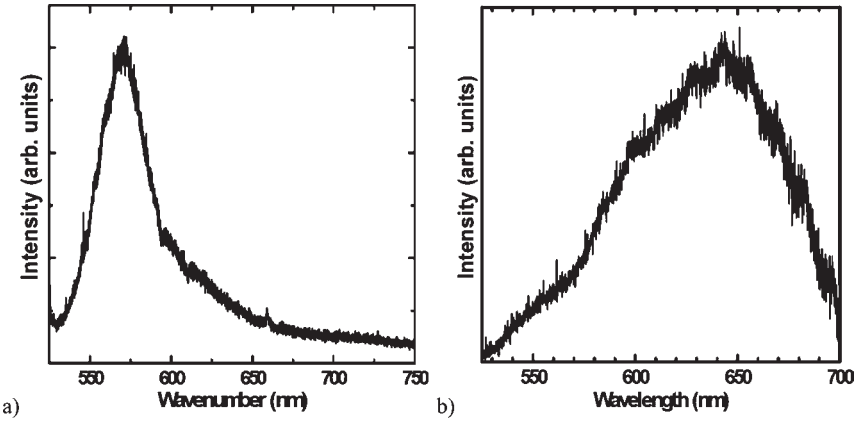

Figure 7. PL of (a) POC and (b) PO powders.

oxygen, further corroborating that the synthesized material is POC. HRTEM measurements demonstrate a good crystalline order inside the POC particles. The particles exhibit clearly resolved lattice fringes with an interplanar spacing of 0.32 nm, assigned to the (101) plane of the POC structure, indicating the formation of hexagonal POC crystals, in agreement with the XRD pattern. The electron diffraction pattern (Figure 5f) presents a unique crystalline orientation.

PO particles obtained after combustion of the as-prepared POC are shown in Figure 6a,b with different resolution. Morphologically, there is not a noticeable change. Round-shaped particles of ~100−200 nm linked together were observed. The EDS of PO depicted the composition of praseodymium and oxygen only (Figure 6c). The elemental analysis further confirms that the oxycarbonate entirely converted into PO during combustion, in agreement with the XRD and IR and Raman spectroscopy measurements.

The room temperature PL spectra obtained from POC and PO is displayed in Figure 7a,b, respectively. POC depicts a visible greenish-yellow luminescence, which consisted of a wide emission band centered at ~570 nm starting at 530 and ending in an asymmetric tail between 600 and 650 nm, a similar emission in the blueish-green is reported for fluorite-type powders.[11] The broad band observed is not the characteristic intense red emission band at 649 nm corresponding to the Pr^{3+} f−f transitions in the visible.[33] Large amounts of surface defects such as dangling bonds, at the interface of nanomaterials, generate additional energy levels in the band gap.[34] The e−h recombination at these centers leads to the greenish-yellow emission in the POC powder. The PL spectrum of the PO (Figure 7b) demonstrates a broad deep-level red emission band from 550 to 700 nm.

(33) Logvinovich, D.; Arakcheeva, A.; Pattison, P.; Eliseeva, S.; Tomes, P.; Marozau, I.; Chapuis, G. *Inorg. Chem.* **2010**, *49*, 1587.
(34) Pol, V. G.; Calderon-Moreno, J. A.; Thiyagarajan, P. *Langmuir* **2008**, *24*, 13640.

Conclusions

The autogenic thermolysis of praseodymium acetate is a solvent-free, efficient, and straightforward approach for the rare synthesis of luminescent POC nanoparticles; the distinctive Raman spectrum of praseodymium oxycarbonate is reported. The as-prepared POC nanopowder converted to the PO powder via combustion, as shown by the methodical morphological, structural, and compositional characterizations of POC and PO powders, supported by mechanistic elucidation.